Int. J. Electrochem. Sci., 14 **(2019)** 9468 – 9481, doi: 10.20964/2019.10.04

International Journal of
ELECTROCHEMICAL
SCIENCE
www.electrochemsci.org

Dissolution of Iron and Ionisation of Hydrogen in Borate Buffer under Cyclic Pulse Polarisation

A.I. Marshakov[*], *A.A. Rybkina*

A.N. Frumkin Institute of Physical Chemistry and Electrochemistry, Russian Academy of Sciences, Moscow, Russia
[*]E-mail*:* mar@ipc.rssi.ru

Received: 4 July 2019/ *Accepted:* 7 August 2019 / *Published:* 30 August 2019

The dissolution of iron in a neutral borate buffer under cyclic pulse polarisation was studied. If the potential is cycled between the values that correspond to the pre-passivity of iron and cathodic hydrogen evolution, the rate of metal dissolution decreases while the external anodic current increases with the frequency and amplitude of the signal. We consider the reasons for which the anodic current changes with time after the potential is switched and show that the initial segments of current transients correspond to a‘solid-state diffusion–phase-boundary kinetics, mixed rate control’mechanism of hydrogen extraction from the metal. The assumption is made that the decrease in the iron dissolution rate under the cyclic pulse polarization is due to the inhibiting effect of atomic hydrogen.

Keywords: dissolution of iron, ionization of hydrogen, potential pulse, chronoamperometry

1. INTRODUCTION

Corrosion of carbon and low-alloy steels under the effect of alternating current (AC corrosion) is among the most hazardous types of corrosion-related destruction of metal structures operating in soil and natural waters. It was believed that the high rates of AC corrosion of those steels were due not only to iron dissolution during the AC anodic half-period but also to the reactions occurring during the cathodic half-period. The latter effect may be caused by various processes: 1) reduction of the passive film that is formed during the AC anodic half-period to iron hydroxides during the cathodic half-period, as a result of which a layer of metal corrosion products is built up [1]; 2) metal passivation under the effect of cathodic potentials (so-called cathodic passivation [2]) followed by pitting [3]; 3) hydrogen charging of the metal that may cause disintegration of iron in the acid [3] or accelerated electrochemical dissolution of iron [5, 6],carbon steels and microalloyed steels [7–12] in near-neutral pH environments; and 4) chemical dissolution of the metal in a highly alkaline environment to give

ferrate anions FeO_4^{2-} [13]. The very list of possible reasons for AC corrosion shows that the kinetics of AC corrosion may be rather involved, and its mechanism has not yet been reliably established.

Studying the mechanism of metal corrosion under the effect of sinusoidal AC is complicated by the presence of its capacitive component. The Faraday component usually makes up a small fraction (several percent) of the effective amperage of industrial-frequency AC [14], the electrode capacity being dependent on a number of factors: duration of experiment [15] and AC and DC amperage (or voltage) [16]. It is reasonable in this context to study the effect of the reactions that occur during the AC cathodic half-period on the dissolution of the metal during the anodic half-period using the rectangular cyclic pulse polarisation (CPP).

Borate buffer is a model solution for studying the kinetics of ionisation of iron and its alloys in neutral environments, since using that solution enables one to avoid a number of problems related to changes in near-electrode pH at potentials of anodic dissolution of metals. The range of potentials more negative than the critical potential of iron passivation in borate buffer is often referred to as the region of active dissolution of the metal. It has been noted, however, that the electrode surface is partially covered with iron oxides or hydroxides at those potentials [17–19], and this range of potentials may be considered as the region of pre-passivation [6, 17, 20] or primary passivity of metals [17, 21].

The electrochemical quartz crystal resonator technique and pulsed chronoamperometry were used to study the kinetics of the initial stages of iron dissolution and passivation in borate buffer (pH 6.7 and 7.4) at pre-passivation potentials [22]. It was shown that a primary passive film was formed on the electrode after preliminary cathodic polarization; the average thickness of that film is as large as several oxide/hydroxide monolayers at a less negative (–0.3 V_{SHE}) potential and no thicker than a single monolayer at a more negative potential (–0.4 V_{SHE}). A continuous barrier layer of oxide is not formed and iron dissolves; the contribution of the latter reaction to the total anodic process increases with time. An increase in the concentration of hydrogen in the metal leads to inhibition of the active dissolution of iron [4, 22] but prevents the formation of the surface layer of oxide/hydroxide compounds [22, 23]. As a result, absorbed hydrogen decreases the anodic current in the initial period of time, but further accelerates metal dissolution. Consequently, the product of the cathodic reaction – atomic hydrogen – can ambiguously affect the rate of iron dissolution in different periods of time during a potential pulse.

The absorbed hydrogen can be ionized at potentials of anodic dissolution of iron in neutral electrolytes, and this phenomenon should also be taken into account in exploring the reactions that occur during the CPP anodic half-period. It was hypothesized that desorption of H atoms from the metal increases the imperfections in its surface layer and facilitates local corrosion of pipe steel under potential fluctuations [24]. Cyclic pulse polarization enables one to accumulate in solution the amount of iron ions that is sufficient to determine the rate of its dissolution by analytical methods. The metal dissolution kinetics can be studied alongside other electrochemical reactions that occur concurrently.

The main goal of this study was to explore the dissolution of iron in a neutral borate buffer under the effect of cyclic potential pulses with various amplitudes and frequencies. Regularities in the time behavior of the external anodic current have been studied for various potential pulse amplitudes.

2. EXPERIMENTAL

Experiments on a rotating (680 rpm) disc electrode (RDE) were performed to determine the external anodic currents and to compare them with the dissolution rates of iron determined by analyzing the metal ions in solution. The anodic current transients were measured on a membrane electrode. Both the RDE and membrane were made of iron with a carbon content of less than 0.01 mass %.The foil for the membranes was annealed at 850 °C for 1 h in argon atmosphere. An auxiliary Pt-electrode and a saturated AgCl reference electrode were used in both series of experiments. Potentials are presented with respect to a standard hydrogen electrode (SHE).

The borate buffer (0.4 M H_3BO_3 + 5.5 mM $Na_2B_4O_7$, pH 6.7) was deaerated with argon. The solution was prepared from reagent grade chemicals using double-distilled water. Experiments were conducted at room temperature 22 ± 2 °C.

The RDE work surface (1.13 cm^2) was ground with SiC up to #600 grit, rinsed with deionized water, dried, and degreased with acetone. The electrode was immersed in the electrolyte solution and then polarized at a potential of $-0.65 V_{SHE}$ for 10 min to remove the air-formed oxide film from the surface. The electrochemical measurements were performed in a three-electrode cell with separated anodic and cathodic spaces using an IPC-Pro MF potentiostat (Cronas Ltd., Russia).

Anodic potentiodynamic curves (0.5 mV/s) were recorded from the free corrosion potential of iron, $E_{cor} \approx -0.49$ V_{SHE}. The value of E_c under cyclic potential pulse ($E_c \leftrightarrow E_a$) was more negative. The time required to impose the potential to within 1 mV was no more than 5×10^{-4} s. The CPP frequency (f) was 50, 5 or 0.5 Hz. The durations of the cathodic (τ_c) and anodic(τ_a) half-periods were equal: $\tau_c = \tau_a = 0.5 f$. The amount of electricity passed during the anodic CPP (q_a) half-period was measured, and the average anodic current was calculated as $i_{a,m} = q_a/\tau_a$.

The mass of dissolved iron was determined by photocolorimetric analysis of electrolyte samples by the 1,10-phenanthroline procedure at a wavelength of 510 nm [25] using a Spekol 211 spectrometer (Carl Zeiss Industrielle Messtechnik GmbH, Germany).

The experiments in which the anodic current transients were obtained were conducted in a Devanathan-Stachurski cell [26] using 100-μm thick membranes with a work area of 2.7 cm^2. A constant cathodic current (i_H) was applied to one side of the membrane (hydrogen charging side) placed in 0.5 M H_2SO_4 solution. Single pulses were applied to the other side of the membrane, changing the potential from various initial E_c values (τ_c = 600 s) to $E_a = -0.3$ V_{SHE} at which anodic current transients were recorded. A more detailed description of membrane preparation and experimental procedure may be found in [4, 27].

3. RESULTS AND DISCUSSION

Figure 1 shows the anodic potentiodynamic curve for iron in borate buffer. The rates of transfer of Fe^{2+} ions into the solution (i_{Fe}) determined at constant potential (E) by colorimetry (Fig.1, red points) virtually coincide with the anodic curve obtained in the region of potentials more negative than the critical passivation potential, which is approximately –0.15 V. The values of i_{Fe} at E= –0.1 and 0 V are smaller than the external anodic currents recorded in the potentiodynamic curve; this implies,

therefore, that a significant fraction of the anodic current corresponds to metal oxidation with formation of a surface layer of iron oxides/hydroxides [22].

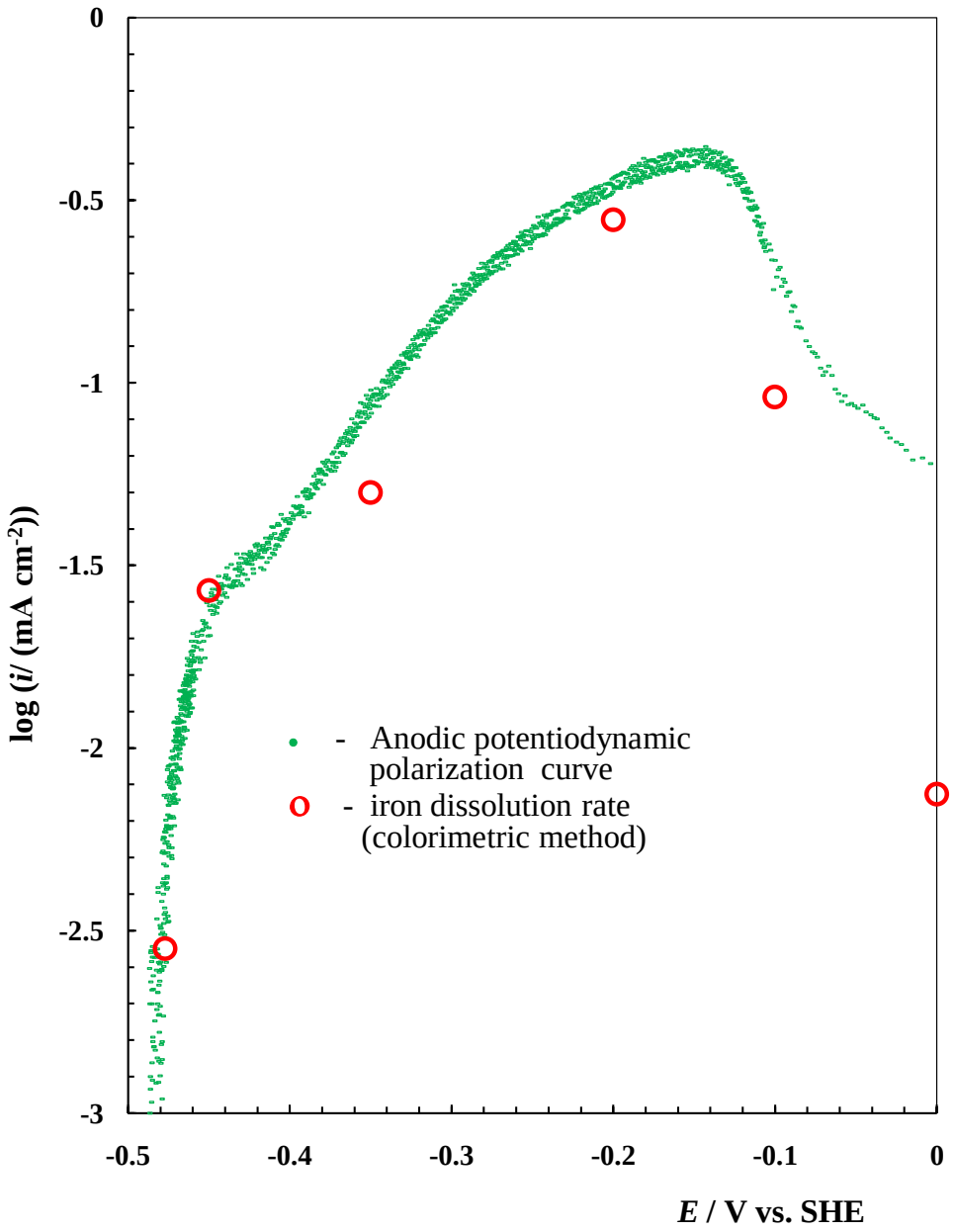

Figure 1. Anodic potentiodynamic curve and iron dissolution rates determined using the colorimetric method in pH 6.7 borate buffer.

Let us consider how the dissolution rate of iron changes upon rectangular cyclic pulse polarization ($i_{Fe,imp}$) depending on the potential of the anodic half-period (E_a).The cathodic half-period potential (E_c) was kept constant and equaled –0.6 V. At this value of E_c, the value of i_{Fe} was less than 0.01 mA/cm^2; therefore, when calculating $i_{Fe\ imp}$, the rate of iron dissolution during the cathodic half-period can be neglected. Since $\tau_a = \tau_c$, to compare the iron dissolution rates at constant E_a and CPP,

$i_{Fe,imp}$ was calculated as $i_{Fe,imp} = 2 \times i_{Fe,ex}$, where $i_{Fe,ex}$ is the dissolution rate of iron under CPP determined by colorimetry.

Table 1 shows $i_{Fe,imp}$ under CPP with a frequency of 50 Hz ($\tau_a = \tau_c = 10^{-2}$ s). One can see that the dissolution rate under CPP changes insignificantly for various values of E_a with E_c = –0.6V; it may, however, differ significantly from i_{Fe} for a given value of E_a (Table 1). The dissolution rate at potentials in the passive (E = 0 V) and active-passive transition ranges (E = –0.1 V) is smaller than $i_{Fe,imp}$ under CPP whereas, quite the opposite, $i_{Fe}/i_{Fe,imp}$ is > 1 in the pre-passivation range of potentials (E = –0.3 V). The current in the anodic half-period ($i_{a,imp}$) has the maximum value at E_a = 0 V (at E_c = –0.6 V) and diminishes as E_a becomes more negative, while $i_{Fe,imp}/i_{a,imp}$ increases (Table 1).

The acceleration of the dissolution of iron and steel under alternating polarisation (alternating sinusoidal or rectangular current) when the value of E reaches the potentials of metal passivation was observed repeatedly [13–16]. This effect is associated with a sufficiently slow passivation process, with the result that during the anodic half-period a significant amount of metal passes into solution, along with the electroreduction of the oxide layer during the cathodic half-period. The fact that the external anodic current exceeds the metal dissolution rate ($i_{Fe,imp}/i_{a,imp} < 1$) shows that a layer of iron oxides/hydroxides is build up on the metal surface at E_a = 0 and –0.1 V.

Table 1. Iron dissolution rate ($i_{Fe,imp}$), average value of external current during the CPP anodic half-period ($i_{a,imp}$), and their ratio for various values of E_a and E_c. The CPP frequency is 50 Hz.

E_a, V	E_c, V	i_{Fe} at E_a, mA/cm^2	$i_{Fe,imp}$, mA/cm^2	$i_{Fe}/i_{Fe,imp}$	$i_{a,imp}$, mA/cm^2	$i_{Fe,imp}/i_{a,imp}$
0	–0.6	0.006	0.085	0.07	1.01	0.08
–0.1	–0.6	0.090	0.120	0.75	0.71	0.17
–0.3	–0.6	0.156	0.113	1.38	0.60	0.19
–0.3	–0.8	0.156	0.10	1.56	1.50	0.07
–0.3	–1.05	0.156	0.02	7.43	2.30	0.01

The iron dissolution rate under CPP with E_a = –0.3 V is smaller than that for the given constant potential while the $i_{Fe,imp}/i_{a,imp}$ ratio is smaller than 1. To study this effect in more detail, let us consider the variation in $i_{Fe,imp}$ as a function of the CPP cathodic half-period potential and frequency (f).

Figure 2 shows how the iron dissolution rate changes as a function of CPP frequency at E_a = –0.3 V and various values of E_c. The value of i_{Fe} at constant E = –0.3 V is shown in Fig. 2 for f = 0. One can see that $i_{Fe,imp}$ diminishes as the frequency increases, while E_c shifts to more negative values. For example, if E_c = –1.05 V and f = 50 Hz, the metal dissolution under CPP is slowed down by a factor of 7.43 (Table 1). At the same time, the external anodic current increases as the CPP frequency increases and cathodic potentials decrease; the ratio $i_{Fe,imp}/i_{a,imp}$ consequently diminishes. For example, $i_{Fe,imp}/i_{a,imp}$ = 0.01 under CPP (50 Hz, E_c = –1.05 V, E_a = –0.3 V).

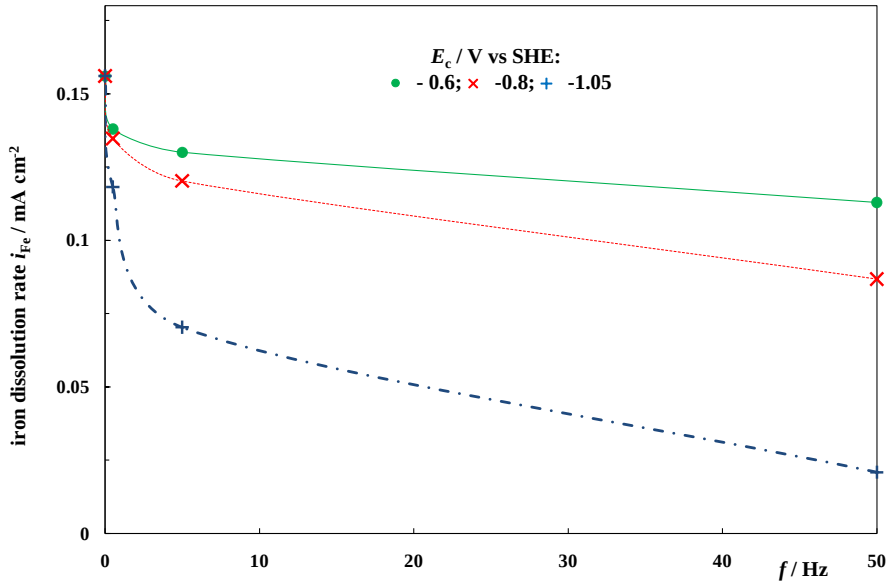

Figure 2. Iron dissolution rate as a function of CPP frequency at E_a = –0.3 V and various E_c in the pH 6.7 borate buffer.

The observed effects might be explained by the cathodic iron passivation phenomenon [2]. Cathodic metal passivation, which is however a consequence of an increase in the pH of the near-electrode electrolyte layer, is observed in a non-buffered solution [3]. A surface layer of iron oxides/hydroxides is formed in the borate buffer (primary passivity) at E = –0.3 V, and this effect is manifested as a sharp decrease in the anodic current in a time interval of 1 – 10 s [22, 28]. The anodic current transients have been obtained on the membrane electrode for a single potential pulse from E_c = –0.55 and –0.6 V to E_a = –0.3 V [22, 28]. The anodic current was shown to change insignificantly in the τ = 0.1 – 1 s interval. A stationary current is established on the hydrogen-charged membrane at τ >1 s, which is equal to the rate at which iron ions pass into the solution [28]. The value of i_a on hydrogen-charged iron at shorter times (τ < 1 s) is larger than the stationary value [28].

To understand the nature of the anodic current at short times after the potential is switched from the cathodic to the anodic value, experiments were made on the membrane electrode. The anodic current transient was recorded on the working side of the membrane, and the hydrogen charging side was polarised with a constant cathodic current i_H. Figure 3 shows anodic current transients in the log i_a–log τ coordinates for a single potential pulse from E_c = –0.8 V to E_a = –0.3 V if the membrane is not charged with hydrogen; i.e., for i_H = 0, and for i_H = 0.71 and 7.41 mA/cm^2. One can see that the anodic current on the hydrogen-charged membrane is greater and increases with i_H.

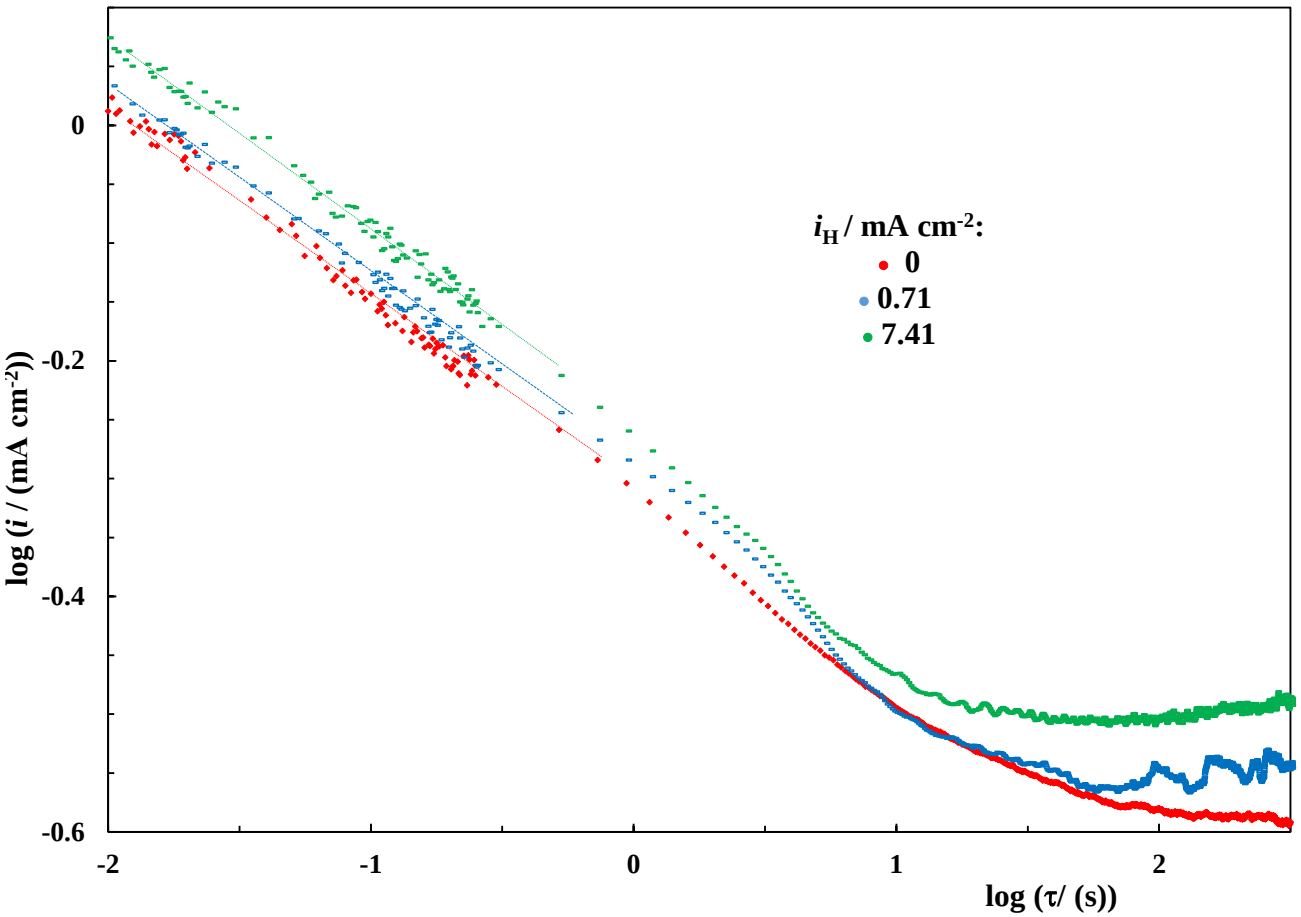

Figure 3. Anodic current transients under a single potential pulse from E_c = –0.8 V to E_a = –0.3 V with various i_H, in the pH 6.7 borate buffer.

Comparison of the current transients obtained for the same E_a = –0.3V but after the potential was switched from various E_c values, –0.6 V [28] and –0.8 V (Fig. 3), shows the following. The shapes of the current transients are approximately the same at τ > 10 s; namely, stationary anodic currents are established on the hydrogen-charged membrane that are larger than i_a for iron not charged with hydrogen (Fig. 3). The effect of hydrogen on the anodic current at shorter times differs: the current on the hydrogen-charged membrane after the potential is switched from E_c = –0.6 V is smaller than in the case without hydrogen charging[22], while the opposite effect is observed if the potential is switched from E_c = –0.8 V.

Figure 3a displays current transient fragments (0.01 s < τ <0.3 s) in the i_a – log τ coordinates. After the 100-μm thick iron membrane was polarised with the cathodic current i_H = 7.41 mA/cm^2, the limiting diffusion flux of hydrogen through the membrane was determined (in current units, $i_{p,H}$) to be 0.12 mA/cm^2 [29]. Straight lines *1* and *2* in Fig. 3a are plotted in such a way that the distance between the lines along the ordinate axis corresponds to $i_{p,H}$ = 0.12 mA/cm^2. One can see that the experimental values of i_a obtained for i_H = 7.41 mA/cm^2 coincide satisfactorily with line *2*. This implies that the anodic currents on the hydrogen-charged membrane differ from those on the metal without hydrogen charging by the values of $i_{p,H}$.

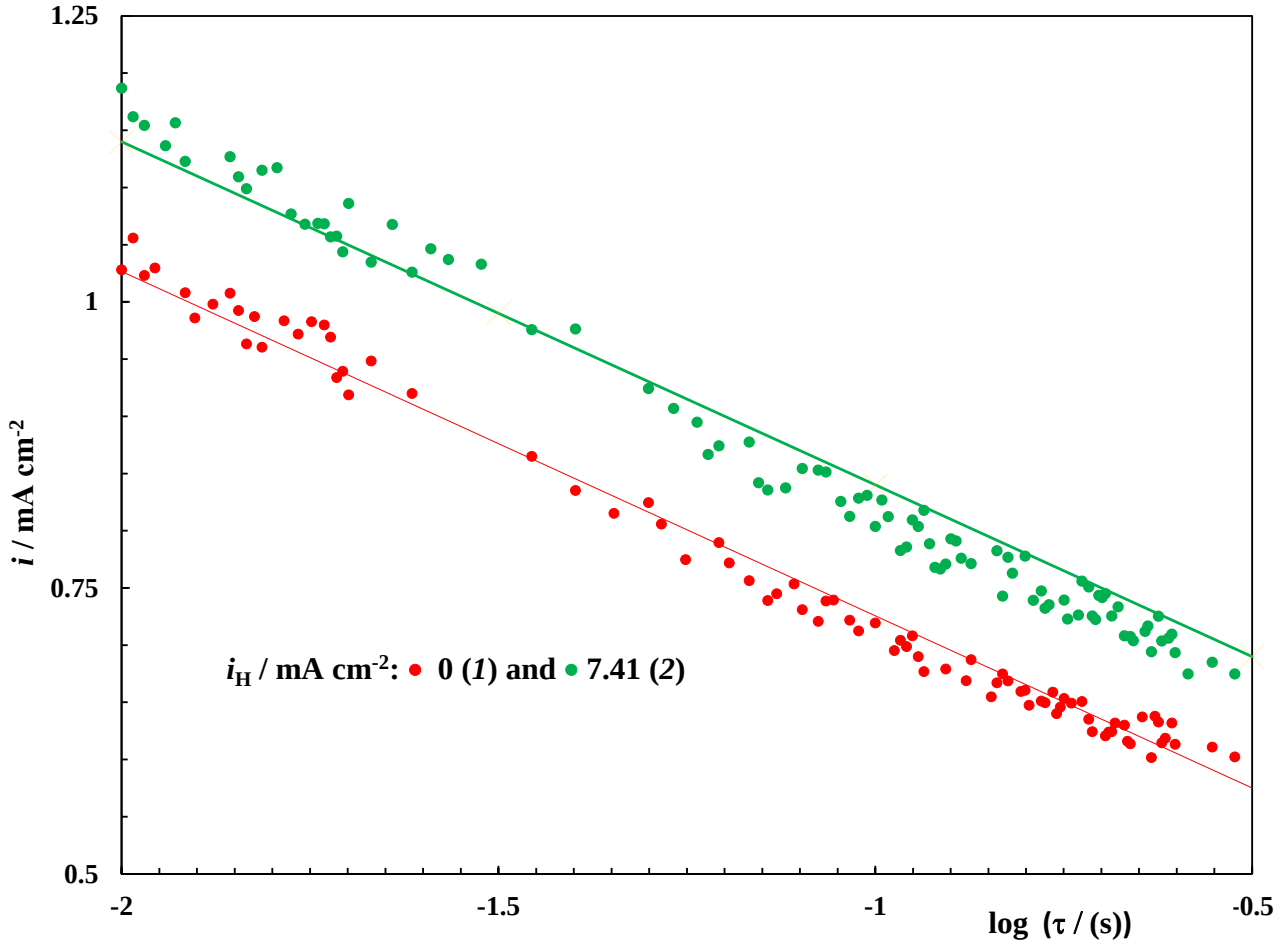

Figure 3a. Fragment of anodic current transients at 0.01 s < τ < 0.3 s under a single potential pulse from E_c = –0.8 V to E_a = –0.3 V with various i_H in the pH 6.7 borate buffer.

One can assume therefore that the atomic hydrogen absorbed by iron at E_c is ionized during an initial period of time after potential switching. The contribution of H atom ionization to the total anodic current apparently depends on both the CPP frequency and the hydrogen concentration in the metal and, hence, on E_c.

Figure 4 shows the log i_a – log τ transients upon potential switching from various E_c to E_a = 0.3 V. The membrane was not charged with hydrogen (i_H = 0). One can see that the anodic current at E_a increases as the potential E_c shifts to the cathodic region. The behavior of the log i_a – log τ transients after cathodic polarization at E_c = –0.5 or –0.6 V coincides with that obtained in [29]: the current decreases in an initial time period (τ <0.1 s); afterwards the time dependence of current is relatively weak (within the interval 0.1 s < τ < 1 s); at τ > 1 s, the slope of log i_a – log τ decreases again, and after ca. 30 s the current becomes virtually constant (Fig. 4). If E_c becomes more negative, the behavior of the anodic current changes: the segment with a small slope in the log i_a – log τ curves disappears in the interval 0.1 s < τ < 1 s. If E_c = –1.05 or –1.2 V, the difference between the log i_a – log τ curves becomes insignificant, and the slope of those segments of the curves in the interval 1 s < τ < 10 s

comes close to 0.5, implying that the $i_a - \tau$ dependence in this time interval is supposed to be linear if expressed in the Cottrell coordinates $i_a - \tau^{-0.5}$.

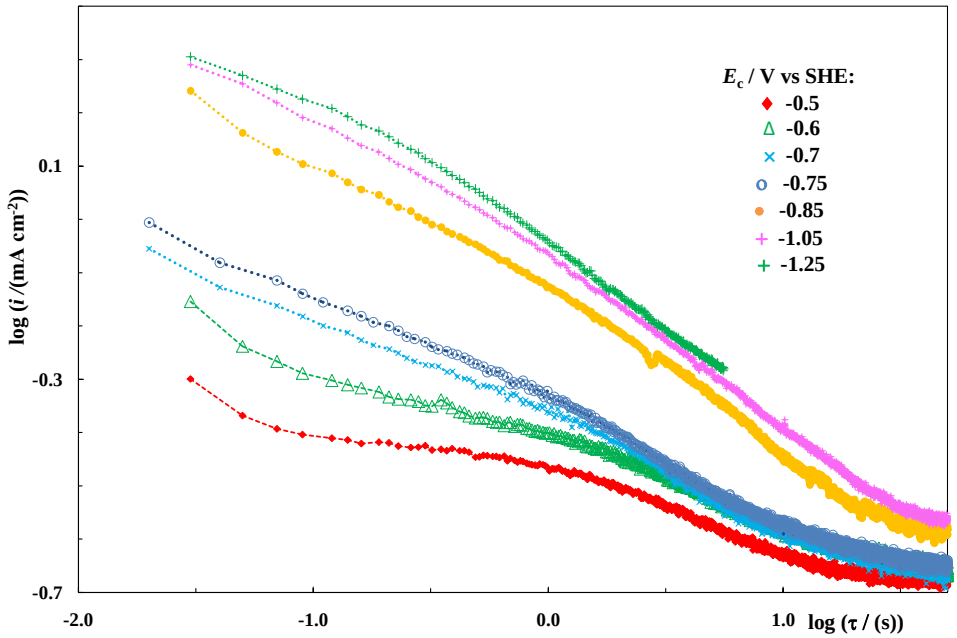

Figure 4. Anodic current transients at E_a = –0.3 V after cathodic polarization at various E_c in the pH 6.7 borate buffer.

It has been shown earlier that the anodic currents for the potential pulse from –0.55 to –0.3 V at $\tau \geq 0.1$ s are determined by the rates of two processes: oxidation of iron with formation of an oxide/hydroxide layer and dissolution of the metal [28]. It was believed that the rate of atomic H ionisation is small under the specified conditions and may be neglected. If the values of E_c are more negative, the concentration of hydrogen absorbed by the metal is supposed to increase and the rate of atomic H oxidation ($i_{H,ox}$) is therefore supposed to increase. The rates of iron oxidation and dissolution should not depend on E_c if the pH of the near-electrode layer in the borate buffer does not increase as E_c diminishes. Hence:

$$i_{H,ox} \approx \Delta i_a = i_{a1} - i_{a2}, \quad (1)$$

where i_{a1} is the anodic current at time τ after switching the potential from the least negative value E_c = –0.5 V, and i_{a2} is the anodic current at the same time τ after switching the potential from the more negative value of E_c.

The greater the difference between the two values of E_c, the more accurately should Δi_a correspond to the rate of oxidation of H atoms at the potential E_a = –0.3 V. Therefore, the current

transients obtained for the potential pulses where $E_c \leq -0.7$ V were used in calculating Δi_a on the basis of Eq. (1).

The $\Delta i_a - \tau$ dependences calculated using Eq. (1) for the anodic current transients shown in Fig. 4 are displayed in Fig. 5 in the coordinates $\Delta i_a - \tau^{-0.5}$. It should be noted that the $\Delta i_a - \tau^{-0.5}$ curves calculated using the current transients for the potential pulses with E_c = –1.05 and –1.25V exhibit linear parts whose extrapolation passes through the coordinate origin (Fig. 5).

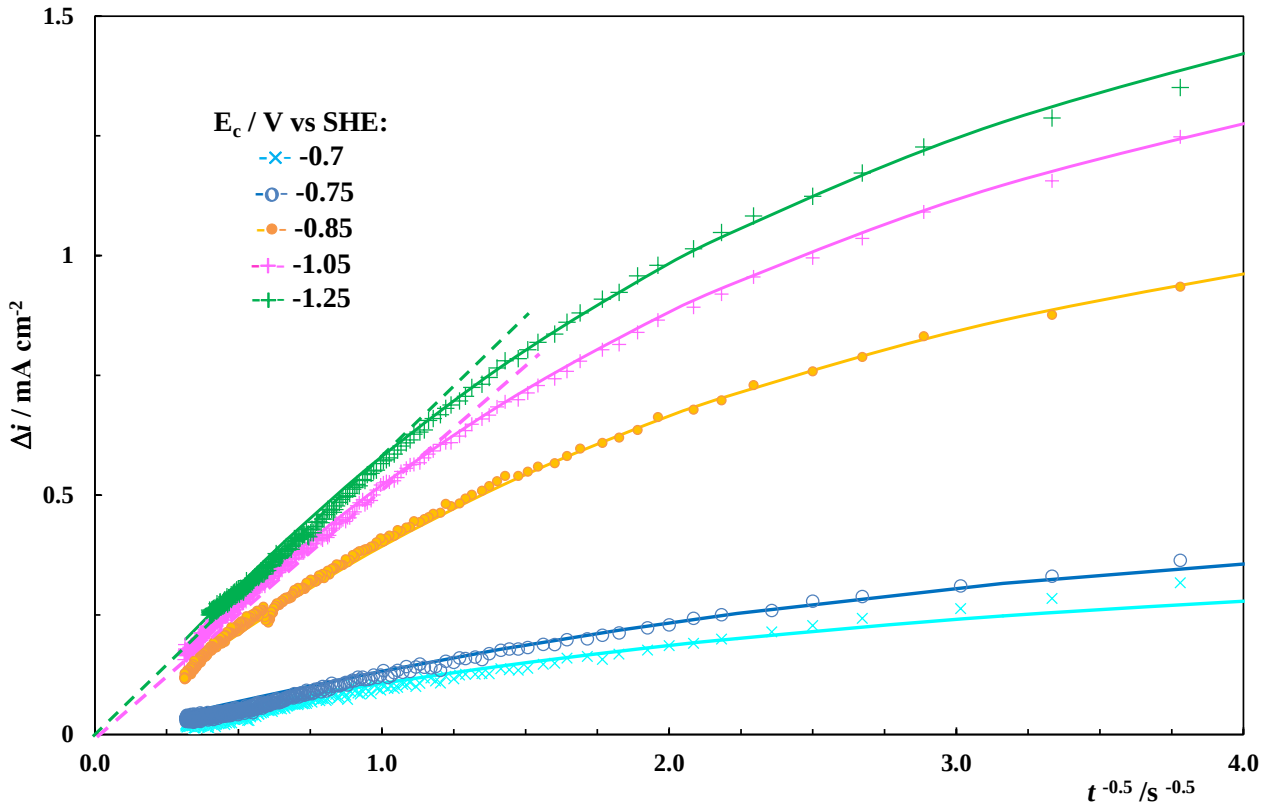

Figure 5. Time dependence of Δi_a for E_a = –0.3 V and various E_c in the pH 6.7 borate buffer.

The initial segment of those curves deviates however from the linear $\Delta i_a - \tau^{-0.5}$ dependence towards smaller currents. As a rule, this effect is associated with kinetic limitations of the reaction rate. For example it has been shown in studies where hydrogen was extracted from palladium and its alloys that desorption of H atoms from the metal phase is the limiting stage of that process at small times, i.e., that the reaction occurs in the phase-boundary kinetics mode [30]. The ionization rate of absorbed hydrogen is limited at longer times by its solid-state diffusion from the bulk of the metal to the phase interface. If oxidation of absorbed H atoms occurs in a mixed mode of solid-state diffusion and phase-boundary kinetics (which is the most general case), then [30]:

$$i_{H,ox}(\tau) = i_{H,ox}^{\infty} - \frac{F(C_H^s - C_H^e)}{\pi^{0.5} t^{0.5}} \times D^{0.5} \times \left(1 - \frac{k\pi^{0.5} t^{0.5}}{D^{0.5}}\right) \exp\frac{k^2 \tau}{D} \operatorname{erfc}\frac{k\tau^{0.5}}{D^{0.5}} \quad (2)$$

where $i_{H,ox}^{\infty}$ is the hydrogen ionization rate at $\tau \to \infty$, C_H^s and C_H^e are the surface and equilibrium hydrogen concentrations in the metal, respectively, k is the phase-boundary constant of hydrogen

desorption rate [30, 31], D is the coefficient of hydrogen diffusion in the metal, and $t = t_c + \tau$ (t_c is the duration of the cathodic polarization of the electrode).

If $t >> \tau$ (this condition is met in our case since t_c = 600s), $i_{H,ox}^{\infty}$ and C_H^e are negligibly small (the stationary anodic current is equal to the iron dissolution rate [29]), and an approximately constant hydrogen concentration $C_H = C_H^s$ is established during the time t_c across the entire thickness of the membrane, so Eq. (2) may be transformed to:

$$i_{H,ox}(\tau) = FC_H k \times \exp\frac{k^2\tau}{D}\operatorname{erfc}\frac{k\tau^{0.5}}{D^{0.5}} \quad . \tag{3}$$

It should be noted that formulas similar to Eq. (3) have been used repeatedly to describe the diffusion-kinetics reaction mode in a semi-infinite diffusion approximation; for example, to describe the time dependence of the dissolution rate of electronegative alloy components in the absence of an interface movement [32].

If $k\tau^{0.5}/D^{0.5} >> 1$, Eq. (3) is simplified to the Cottrell equation:

$$i_{H,ox}(\tau) = \frac{FC_H D^{0.5}}{\pi^{0.5}\tau^{0.5}}, \tag{4}$$

implying that the $i_{H,ox} - \tau$ dependence should be linear in the coordinates $i_{H,ox} - \tau^{-0.5}$ and its extrapolation should pass through the coordinate origin.

After setting $D = 7.3 \times 10^{-5}$ cm^2/s [33], numerical methods were used to determine the values of C_H and k (Table 2) for which the $i_{H,ox} - \tau$ dependences obtained using Eq. (3) (Fig. 5, lines) coincide best with the Δi_a values at $\tau < 10$ s (Fig. 5, points).

Table 2. Hydrogen concentration in iron (C_H) and rate constant of hydrogen desorption from the metal phase (k) determined for potential pulses with $E_a = -0.3$ V and various values of E_c.

E_c, V	$C_H \times 10^7$, mol/cm^3	$k \times 10^2$, cm/s
–1.2	13.6	1.8
–1.05	12.2	1.8
–0.85	9.2	1.8
–0.8	7.8	1.8
–0.75	3.0	2.3
–0.7	2.45	2.1

The k values obtained agree well with the rate constant of hydrogen desorption from iron in 0.1 M NaOH, which is equal to $(1.4 \pm 0.6) \times 10^{-2}$ cm/s [34]. In agreement with expectations, the hydrogen concentration in the metal increases if E_c shifts towards negative values (Table 2). At the same time, the C_H values obtained significantly exceed the C_H values that follow from the calculations under the assumptions of stationary penetration of hydrogen through the iron membrane. For example, the stationary rate of hydrogen penetration (i_p) through a steel membrane (grade 3 steel, thickness $L = 100$ μm) at $E = -1.0$ V in the borate buffer with pH 6.7 is 6 μA/cm^2 [30]. Hence, setting $D = 7.3 \times 10^{-5}$ cm^2/s and using the equation:

$$C_H^{st} = \frac{i_p L}{FD}, \quad (5)$$

we obtain $C_H^{st} = 8.4 \times 10^{-9}$ mol/cm^3, a value that is significantly smaller than the C_H displayed in Table 2.

One may assume that the difference between C_H^{st} and C_H determined under stationary conditions and the potential pulse, respectively, is related to invalidity of the assumption we made that C_H is constant across the entire membrane thickness. Experiments with a membrane made of Armco iron have shown that 97.6 % of the total amount of absorbed hydrogen (q_H) is contained in reversible traps in the metal layer adjoining the cathodically polarized membrane side and, consequently, only 2.4% of q_H can be determined using the standard method of i_p measurement under stationary conditions [35]. At anodic polarization of the entry (hydrogen charging) side of the membrane, H atoms are desorbed from reversible traps resulting in the emergence of an 'excessive' hydrogen ionization current [35]. This phenomenon, which is apparently observed due to the potential pulse effects, results in the difference between C_H and C_H^{st}.

Thus, the analysis of anodic current transients has shown that after the potential is switched, hydrogen desorption from iron should occur during an initial time interval after switching in the mixed mode of solid-state diffusion and phase-boundary kinetics. The near-surface concentration of H atoms in the metal and hence the hydrogen coverage on the iron surface (θ_H) should differ from zero. The θ_H value is supposed to increase at short times ($\tau \to 0$) and if E_c shifts towards negative values. If the surface of the metal is clean, i.e., there is no oxide/hydroxide film on it, growth of θ_H slows down the dissolution of iron [4, 29].

The decrease in the iron dissolution rate if the frequency and amplitude of the CPP increase from E_a = –0.3 V (Fig. 2) is supposed to be related to the inhibiting effect of adsorbed hydrogen. If the CPP frequency and amplitude are small (i.e., E_c is less negative), hydrogen has enough time to desorbs almost completely from the metal and the iron dissolution rate increases, tending to a stationary value (Fig. 2).

It should be emphasised that the effects described above are observed in the buffer solution in the absence of ions that activate the dissolution of iron. In an unbuffered chloride electrolyte, cathodic passivation of carbon steel and formation of pits occur, which accelerate the dissolution of the metal under the action of AC [3]. Studies show that the composition of the corrosive environment plays a prevailing role in the dissolution of the metal under alternating polarization.

4. CONCLUSIONS

The regularities of iron dissolution in a neutral borate buffer under the effect of cyclic pulse polarisation are considered. If the potential is cycled between the two values that correspond to the regions of iron pre-passivity and passivity in a borate buffer, the rate of iron ion passage to the solution exceeds the dissolution rate under stationary conditions. This effect is related to passivation being a rather slow process, owing to which a significant amount of the metal passes into the solution during the anodic half-period. If potential is cycled between two values that correspond to the regions of iron

pre-passivity and cathodic evolution of hydrogen, the iron dissolution rate decreases, and the external anodic current increases with the potential pulse frequency and amplitude. During an initial period of time after the potential is switched, the anodic current on the membrane electrode increases by a value that is approximately equal to the rate of hydrogen penetration through the membrane. The initial segments of the current transients measured on the membrane at various values of the cathodic half-period potential can be described by the equation of 'solid-state diffusion–phase-boundary kinetics, mixed rate control' mechanism of hydrogen extraction from the metal [30]. The rate constant of hydrogen atom desorption from the metal phase has been calculated, and its value agrees well with published data [34]. It was assumed that the decrease in the iron dissolution rate in the neutral borate buffer on increase in the frequency and amplitude of the cyclic potential pulses is related to the inhibiting effect of adsorbed hydrogen on the active dissolution of metal.

References

1. CEN/TS 15280, Evaluation of A.C. corrosion likelihood of buried pipelines - Application to cathodically protected pipelines, Technical Specification, 2006.
2. L.I. Freiman, E.G. Kuznetsova, *Prot. Metals Phys. Chem.Surfaces*, 37 (2001) 537.
3. A.I. Marshakov, T.A. Nenasheva, E.V. Kasatkin, I.V. Kasatkina, I.V., *Prot. Metals Phys. Chem. Surfaces*, 54 (2018) 1236.
4. A.I. Marshakov, A.A. Rybkina, Ya.B. Skuratnik, *Russ. J. Electrochem.*, 36 (2000) 1236.
5. S. Pyun, C. Lim, R.A. Oriani, *Corros. Sci.*, 33 (1992) 437.
6. A.I. Marshakov, M.A. Maleeva, A.A. Rybkina, V.B. Elkin, *Prot. Metals Phys. Chem.Surfaces*, 46 (2010) 40.
7. M.C. Li, Y.F. Cheng, *Electrochim. Acta*, 52 (2007) 8111.
8. Y. Yuan, L. Liang, C. Wang, Y. Zhu, *Electrochem. Commun*., 12 (2010) 1804.
9. Y.M. Zeng, J.L. Luo, P.R. Norton, *Electrochim. Acta*, 49 (2004) 703.
10. J. Cwiek, K. Nikiforov, *Mater. Sci.*, 40 (2004) 831.
11. S. Thomas, N. Ott, R.F. Schaller, J.A. Yuwono, P. Volovitch, G. Sundararajan, N.V. Medhekar, K. Ogle, J.R. Scully, N. Birbilis, *Heliyon*, 3 (2017) e00209.
12. T.A. Nenasheva, A.I. Marshakov, *Prot. Metals Phys. Chem. Surfaces*, 51 (2015) 1018.
13. A. Brenna, L. Lazzari, M. Ormellese, A Proposal of AC Corrosion Mechanism of Carbon Steel in Cathodic Protection Condition, NACE International Conference "Corrosion 2013", Houston, Texas, USA, 2013, paper No. 2457.
14. 14 L.Y. Xu, X. Su, Z.X. Yin, Y.H. Tang, Y.F. Cheng, *Corros. Sci.*, 61 (2012) 215.
15. A.I. Marshakov, T.A. Nenasheva, *Prot. Metals Phys. Chem. Surfaces*, 53 (2017) 1214.
16. L.W. Wang, X.H. Wang, Z.Y. Cui, Z.Y. Liu, C.W. Du, X.G. Li, *Corros. Sci.*, 86 (2014) 213.
17. S.P. Harrington, F. Wang, T.M. Devine, *Electrochim. Acta*, 55(2010) 4092.
18. H. Wroblova, V. Brusic, J.O'M. Bockris, *J. of Phys. Chem.*, 75 (1971) 2823.
19. W.J. Lorenz, G. Staikov, W. Schindler, W. Wiesbeck, *J. Electrochem. Soc.*, 149 (2002) K47.
20. M. Keddam, O.R. Mattos, H. Takenouti, *J. Electrochem. Soc*., 128 (1981) 257.
21. M.E. Garmanov, Yu.I.Kuznetsov, *Prot. Metals Phys. Chem. Surfaces*, 40 (2004) 31.
22. A.I. Marshakov, A.A. Rybkina, L.B. Maksaeva, M.A. Petrunin, A.P. Nazarov, *Prot. Metals Phys. Chem. Surfaces* 52 (2016) 936.
23. S. Modiano, J.A.V. Carreño, C.S. Fugivara, R.M. Torresi, V. Vivier, A.V. Benedetti, O.R. Mattos, *Electrochim. Acta*, 53 (2008) 3670.
24. T.A. Nenasheva, A.I. Marshakov, I.V. Kasatkina, *Corros.: Mat.Prot.*, 5 (2015) 9 (in Russian).
25. Biological Role of Microelements, Ed. V.B. Koval'sky, Nauka (1983), Moscow, 283 (in Russian).

26. M.A.V. Devanathan, Z. Stachurski, *Proceeding of the Royal Society. Ser. A. Mathematical and Physical Science*, 270 (1962) 92.
27. A.I. Marshakov, A.A. Rybkina, T.A. Nenasheva, *Prot. Metals Phys. Chem. Surfaces*, 43 (2007) 605.
28. A.I. Marshakov, A.A. Rybkina, M.A. Maleeva, A.A. Rybkin, *Prot. Metals Phys. Chem. Surfaces*, 50 (2014) 345.
29. M.A.Maleeva, Thesis for the degree of Cand. Sci. (Chemistry), Moscow, 2009, 195 pp (in Russian).
30. N.B. Morozova, A.V. Vvedensky, I.P. Beredina, *Prot. Metals Phys. Chem. Surfaces*, 50 (2014) 699.
31. M. Zamanzadeh, A. Allam, H.W. Pickering, G.K. Hulber, *J. Electrochem. Soc.*, 127 (1980) 1688.
32. A.I. Marshakov, Ya.B. Skuratnik, A.P. Pchel'nikov, V.V. Losev, *Soviet Electrochem*., 22 (1986) 325.
33. K. Kiuchi, R.B. McLellan, *Acta metallurgica*, 31 (1983) 961.
34. R.N. Iyer, H.W. Pickering, M. Zamanzadeh, *J. Electrochem. Soc.*, 136 (1989) 2463.
35. T. Zakroczymski, *Electrochim. Acta*, 51 (2006) 2261.